Supporting Information

Metal-organic-framework-derived N-doped hierarchically porous carbon polyhedrons anchored on crumpled graphene balls as efficient selenium hosts for high-performance lithium-selenium batteries

*Seung-Keun Park, Jin-Sung Park and Yun Chan Kang**

Department of Materials Science and Engineering, Korea University, Anam-Dong, Seongbuk-Gu, Seoul 136-713, Republic of Korea

* Corresponding author: *yckang@korea.ac.kr (Y.C. Kang)*

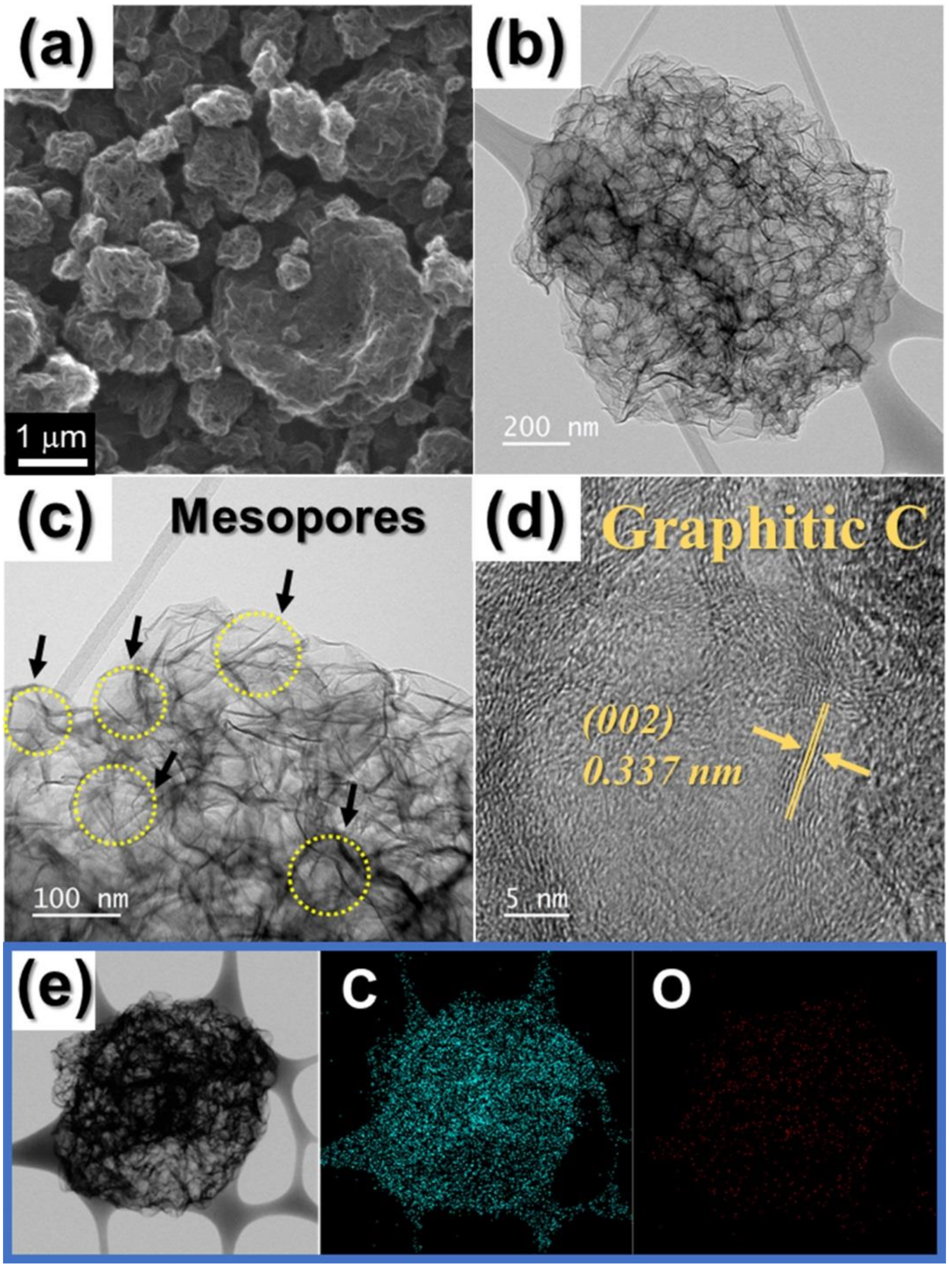

Figure S1. Morphologies, SAED patterns, and elemental mapping images of mesoporous CGB: (a) SEM image, (b and c) TEM images, (d) HR-TEM image, (e) elemental mapping images.

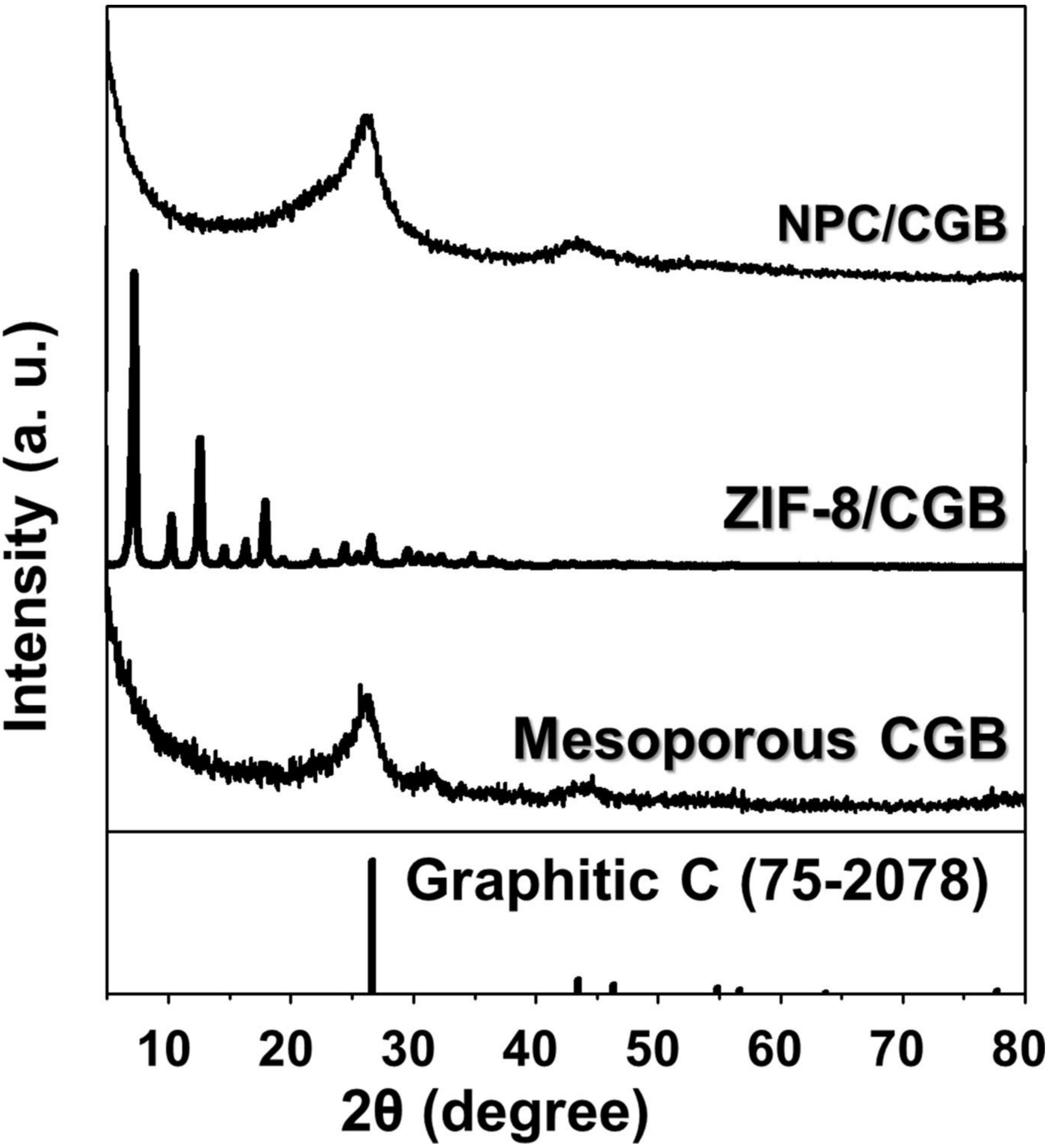

Figure S2. XRD patterns of mesoporous CGB, ZIF-8/CGB, and NPC/CGB.

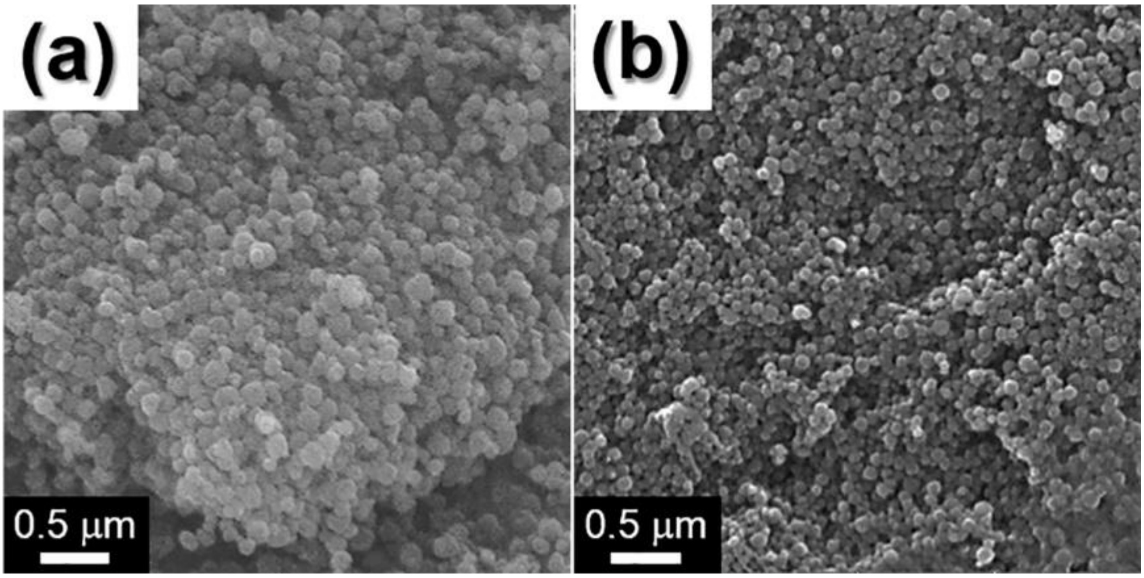

Figure S3. SEM images of ZIF-8 polyhedrons (a) before and (b) after annealing at 900 ºC.

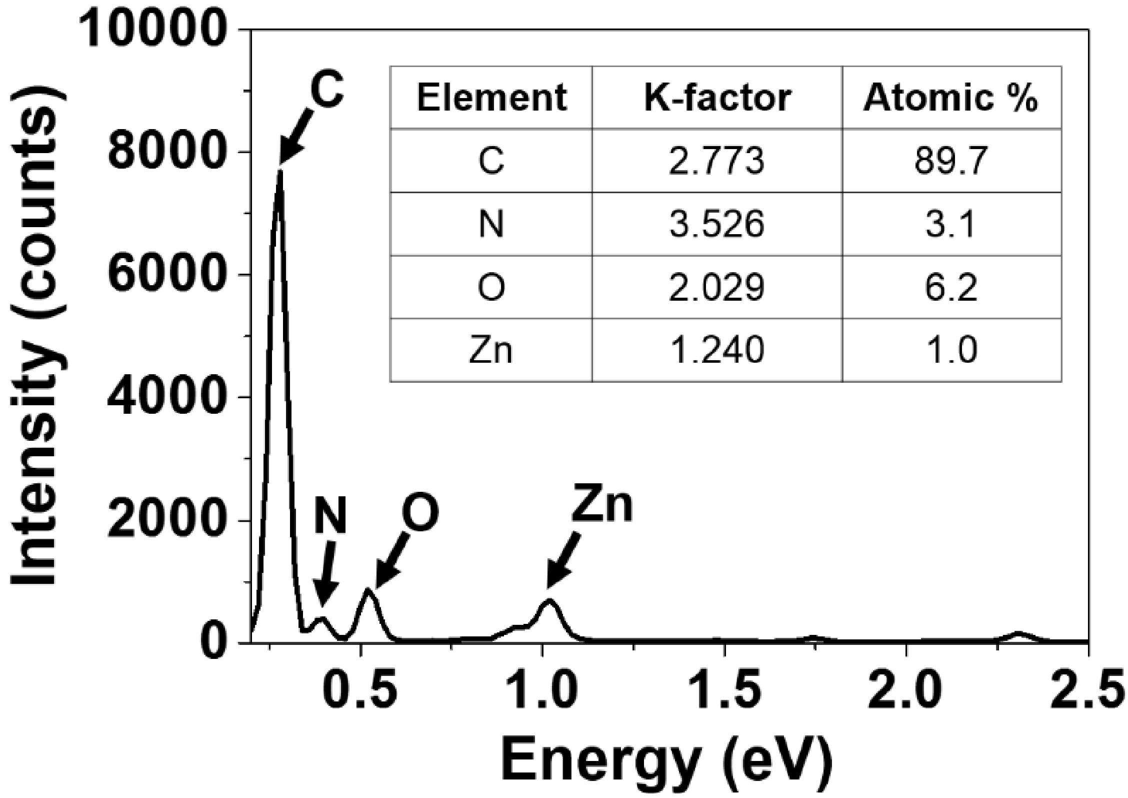

Element	K-factor	Atomic %
C	2.773	89.7
N	3.526	3.1
O	2.029	6.2
Zn	1.240	1.0

Figure S4. EDX spectrum and elemental composition table of NPC/CGC composites.

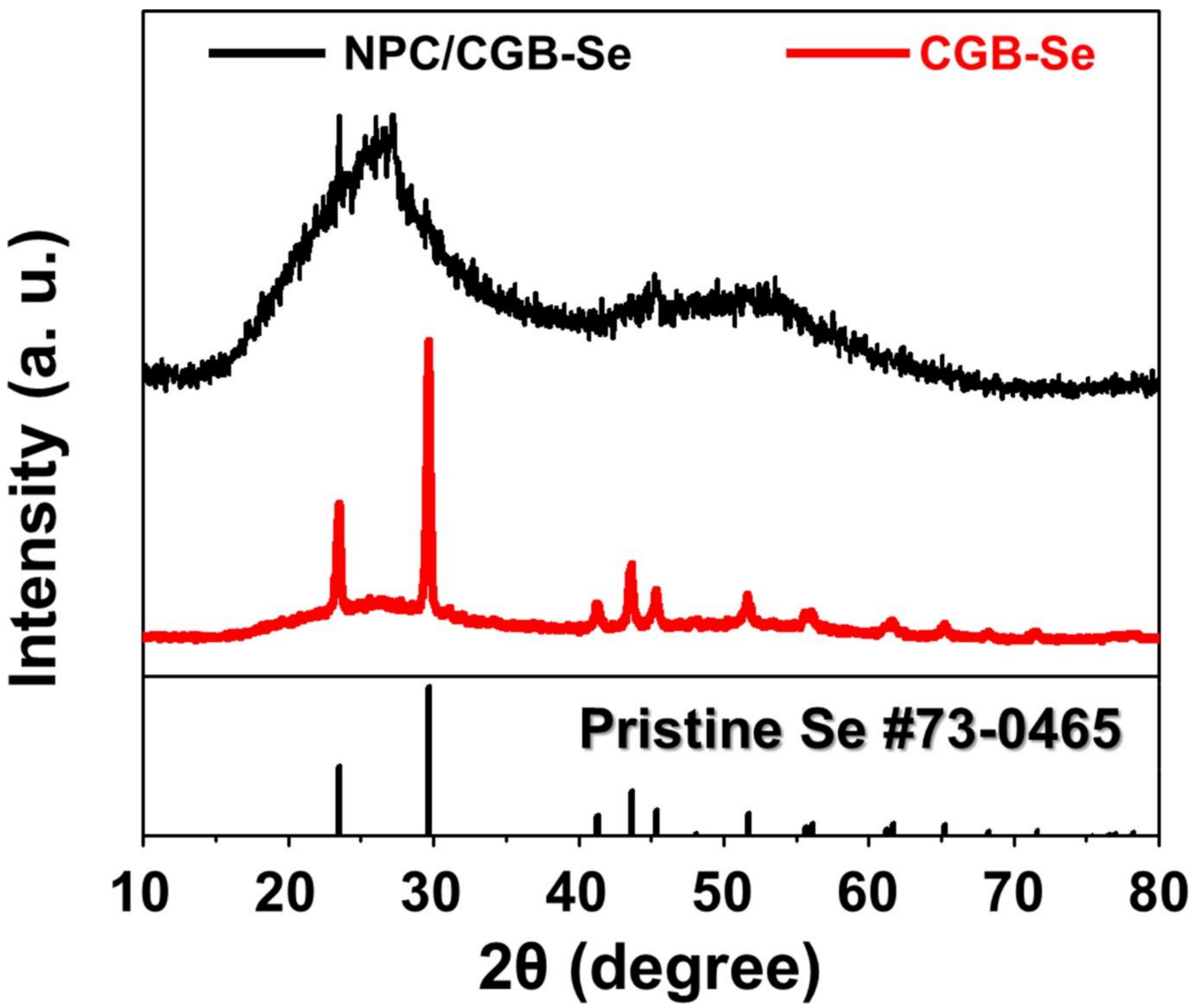

Figure S5. XRD patterns of NPC/CGB-Se and CGB-Se.

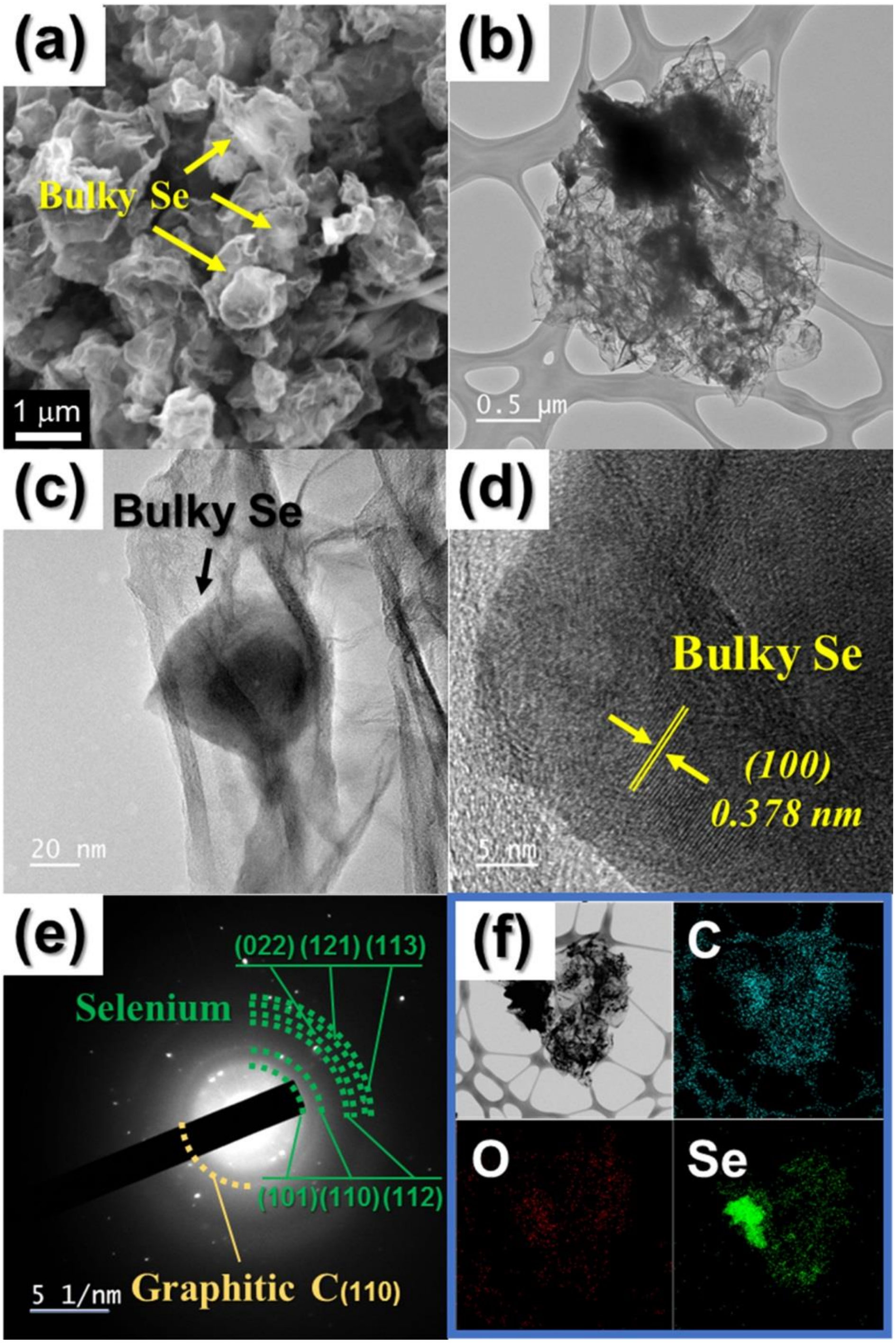

Figure S6. Morphologies, SAED patterns, and elemental mapping images of CGB-Se: (a) SEM image, (b and c) TEM images, (d) HR-TEM image, (e) SAED pattern, and (f) elemental mapping images.

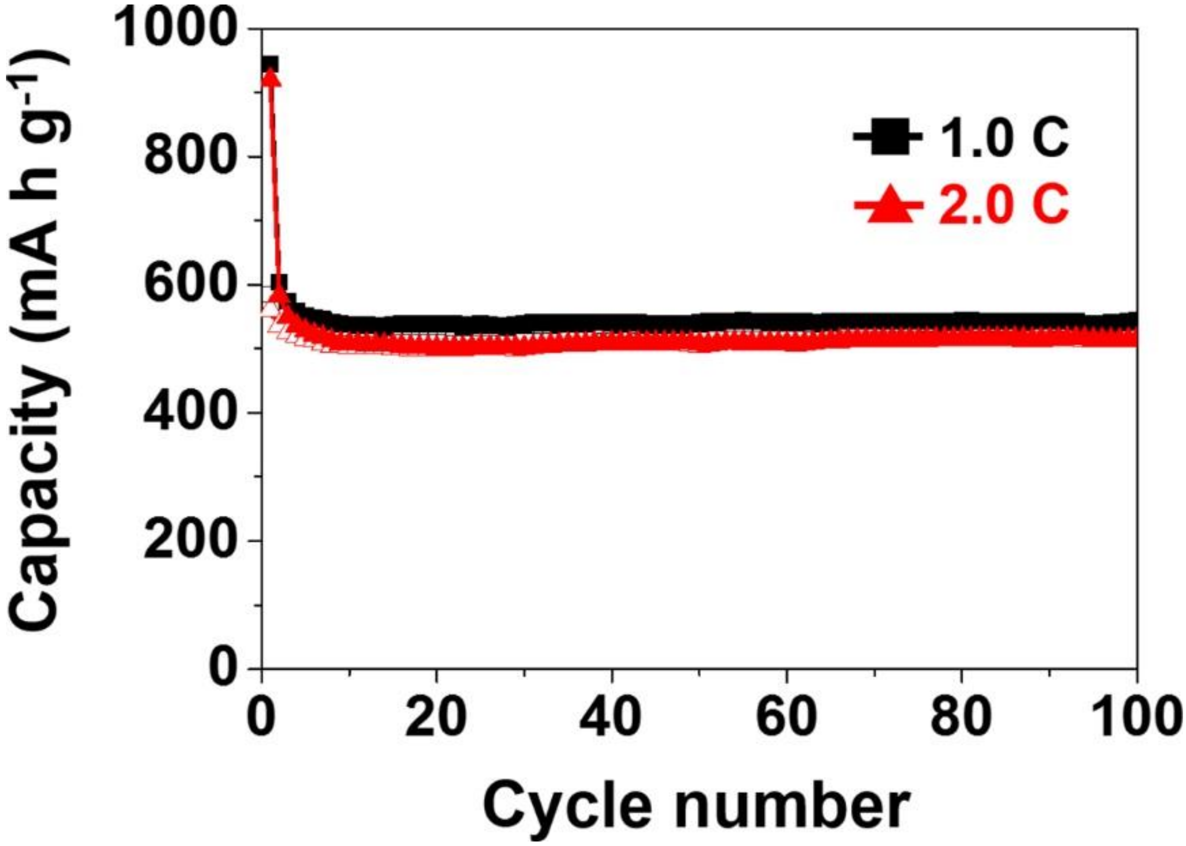

Figure S7. Cycle performances of NPC/CGB-Se at current densities of 1.0 and 2.0 C.

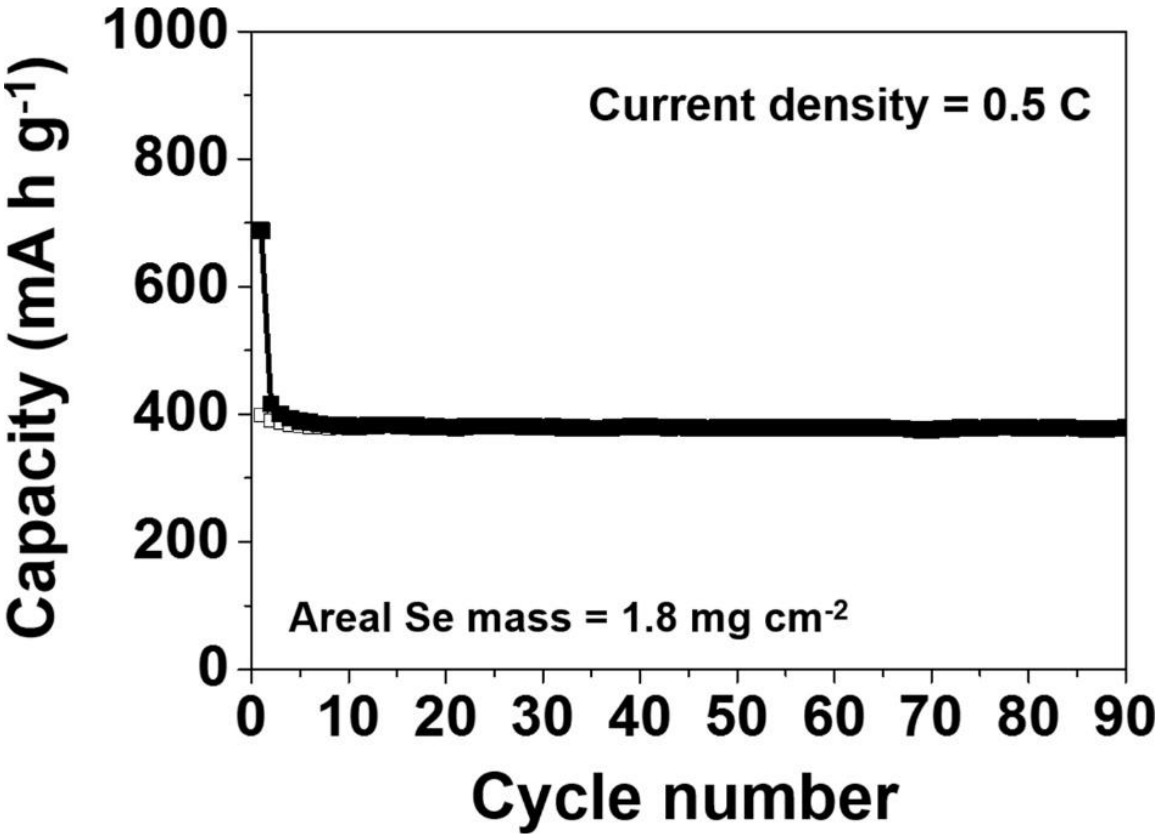

Figure S8. Cycle performance of NPC/CGB-Se with higher areal Se loading at current densities of 0.5 C.

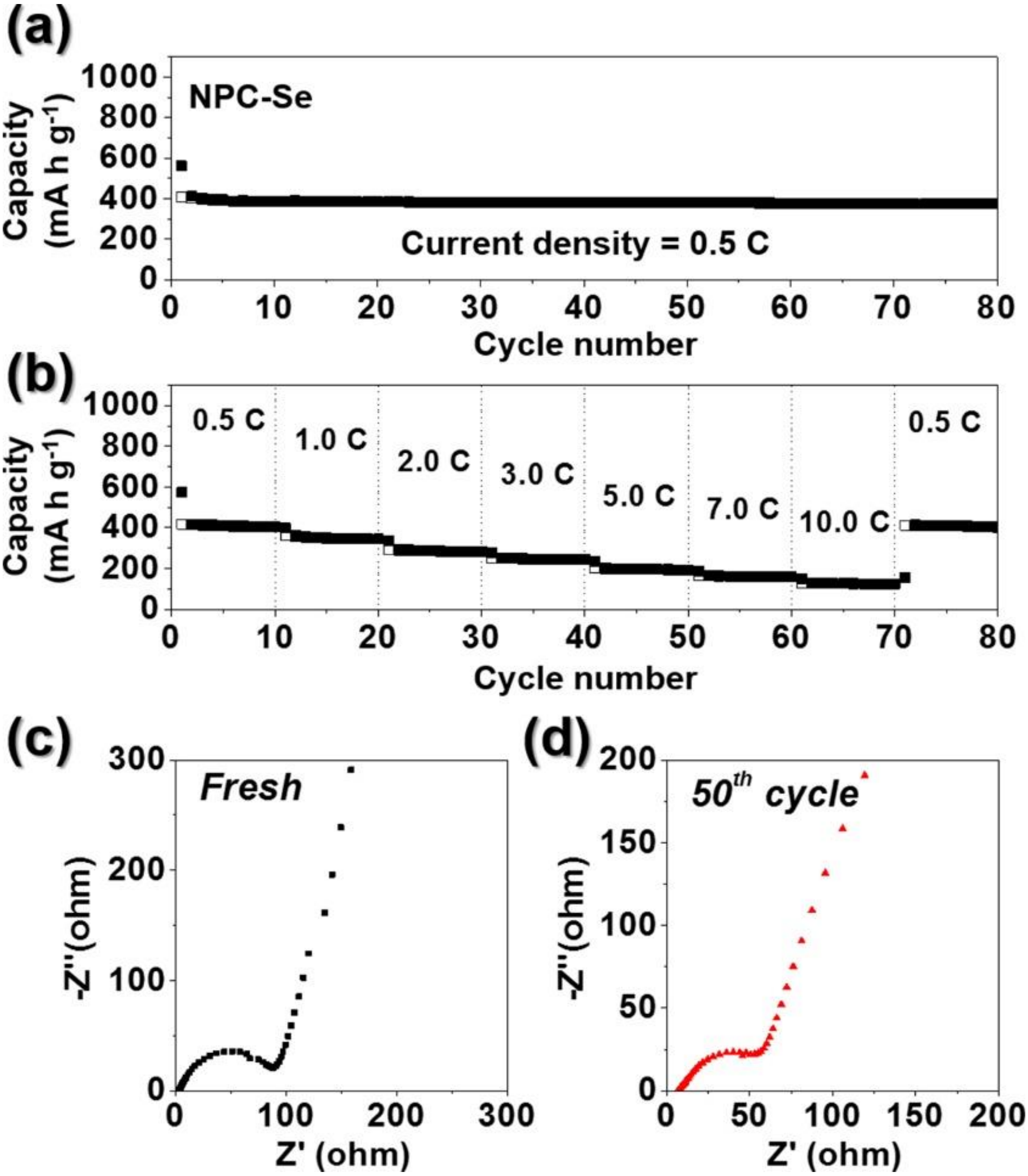

Figure S9. Electrochemical properties of NPC-Se: (a) cycle and (b) rate performances, and Nyquist plot (c) before cycling and (d) after 50 cycles.

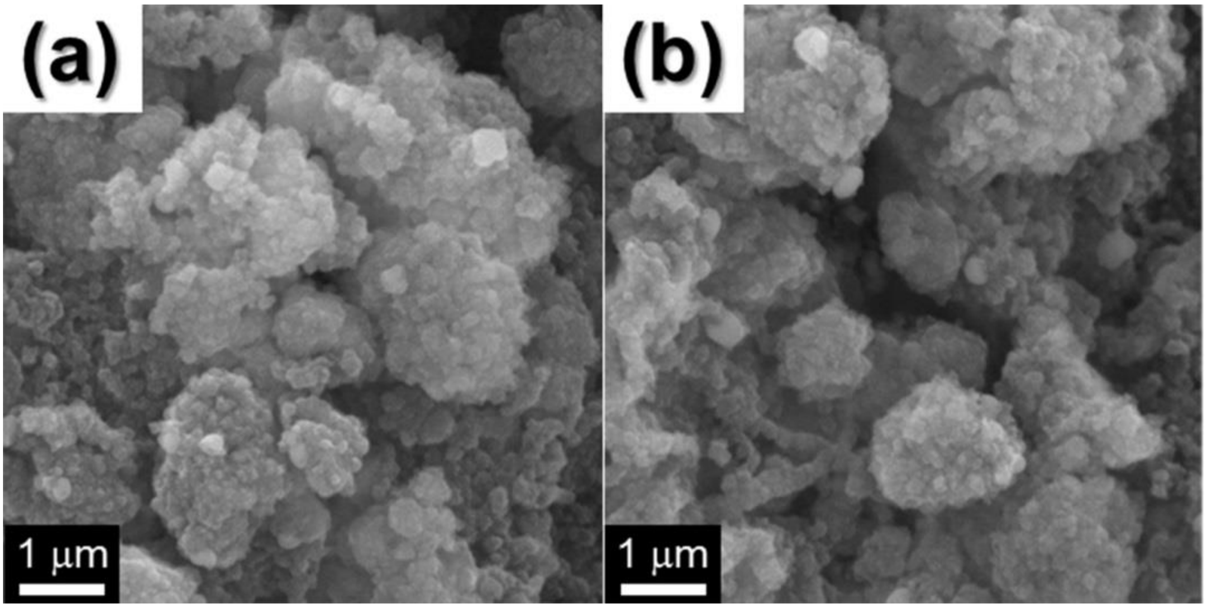

Figure S10. (a, b) SEM images of NPC/CGB-Se after 1000 cycles.

Table S1. Comparison of electrochemical performances of various nanostructured materials used as cathode materials for lithium-selenium batteries.

Morphology [preparation method]	Se content (%)	Current density	Initial discharge /charge capcities [mA h g^{-1}]	Discharge capacity [mA h g^{-1}] and (cycle number)	Rate capacity [mA h g^{-1}]	Ref.
N-doped porous carbon polyhedron anchored on crumpled graphene ball [spray pyrolysis]	**60**	**0.5 C**	**998/659**	**462 (1000)**	**409 (15 C)**	***This work***
3D mesoporous carbon [heating melt-infiltration]	62	0.1 C (first 5 cycles)1 C	655/- 432/-	385 (1300)	274 (3 C)	(1)
metal-organic frameworks derived porous carbon microcubes [hydrothermal]	49.7	0.2 C	974/780	307.6 (460)	218.1 (5 C)	(2)
Metal complex-derived porous carbon [salt-bake approach]	72	0.1 C	904/~635	636 (150)	547 (10 C)	(3)
Three-dimensional hierarchical porous tubular carbon [KOH activation of coconut shell]	53	0.2 C	415/-	317 (900)	325 (2 C)	(4)
Porous carbon nanofiber webs [modified oxidative template assembly]	33.2	1 C	439/-	323.7 (300)	345.6 (1 C)	(5)
Heteroatom-doped microporous carbon [carbonization of polypyrrole with KOH]	60	1 C	~1200/664	506 (150)	303 (20 C)	(6)
Nitrogen-containing hierarchical porous carbon [template-assisted]	56.2	2 C	435/~314	305 (60)	~246 (5 C)	(7)
Porous hollow carbon bubbles [hydrothermal]	~50	0.1 C	691.1/454.6	606.3 (120)	431.9 (1 C)	(8)
Graphene–encapsulated selenium / polyaniline core–shell nanowires [*in situ* chemical oxidative polymerization]	~59.7	0.1 C	917/~708	540 (100)	430 (5 C)	(9)
Carbon bonded and encapsulated selenium composites [*in situ* carbonization]	54	100 mA g^{-1}	862/560	430 (250)	280 (1200 mA g^{-1})	(10)

References

(1) Han, K.; Liu, Z.; Shen, J. M.; Lin, Y. Y.; Dai, F.; Ye, H. Q. A Free-Standing and Ultralong-Life Lithium-Selenium Battery Cathode Enabled by 3D Mesoporous Carbon/Graphene Hierarchical Architecture. *Adv. Funct. Mater.* **2015,** *25*, 455-463.

(2) Liu, T.; Jia, M.; Zhang, Y.; Han, J.; Li, Y.; Bao, S. J.; Liu, D. Y.; Jiang, J.; Xu, M. W. Confined Selenium within Metal-Organic Frameworks Derived Porous Carbon Microcubes as Cathode for Rechargeable Lithium Selenium Batteries. *J. Power Sources* **2017,** *341*, 53-59.

(3) Li, X. N.; Liang, J. W.; Hou, Z. G.; Zhang, W. Q.; Wang, Y.; Zhu, Y. C.; Qian, Y. T. A New Salt-Baked Approach for Confining Selenium in Metal Complex-Derived Porous Carbon with Superior Lithium Storage Properties. *Adv. Funct. Mater.* **2015,** *25*, 5229-5238.

(4) Jia, M.; Lu, S. Y.; Chen, Y. M.; Liu, T.; Han, J.; Shen, B. L.; Wu, X. S.; Bao, S. J.; Jiang, J.; Xu, M. W. Three-Dimensional Hierarchical Porous Tubular Carbon as a Host Matrix for Long-Term Lithium-Selenium Batteries. *J. Power Sources* **2017,** *367*, 17-23.

(5) Zhang, J.; Zhang, Z. A.; Li, Q.; Qu, Y. H.; Jiang, S. F. Selenium Encapsulated into Interconnected Polymer-Derived Porous Carbon Nanofiber Webs as Cathode Materials for Lithium-Selenium Batteries. *J. Electrochem. Soc.* **2014,** *161*, A2093-A2098.

(6) Yi, Z. Q.; Yuan, L. X.; Sun, D.; Li, Z.; Wu, C.; Yang, W. J.; Wen, Y. W.; Shan, B.; Huang, Y. H. High-Performance Lithium-Selenium Batteries Promoted by Heteroatom-Doped Microporous Carbon. *J. Mater. Chem. A* **2015,** *3*, 3059-3065.

(7) Qu, Y. H.; Zhang, Z. A.; Jiang, S. F.; Wang, X. W.; Lai, Y. Q.; Liu, Y. X.; Li, J. Confining Selenium in Nitrogen-Containing Hierarchical Porous Carbon for High-Rate Rechargeable Lithium-Selenium Batteries. *J. Mater. Chem. A* **2014,** *2*, 12255-12261.

(8) Zhang, J. J.; Fan, L.; Zhu, Y. C.; Xu, Y. H.; Liang, J. W.; Wei, D. H.; Qian, Y. T. Selenium/Interconnected Porous Hollow Carbon Bubbles Composites as the Cathodes of Li-Se Batteries with High Performance. *Nanoscale* **2014,** *6*, 12952-12957.

(9) Ye, H.; Yin, Y. X.; Zhang, S. F.; Guo, Y. G. Advanced Se-C Nanocomposites: A Bifunctional Electrode Material for Both Li-Se and Li-Ion Batteries. *J. Mater. Chem. A* **2014,** *2*, 13293-13298.

(10) Luo, C.; Wang, J. J.; Suo, L. M.; Mao, J. F.; Fan, X. L.; Wang, C. S. In Situ Formed Carbon Bonded and Encapsulated Selenium Composites for Li-Se and Na-Se Batteries. *J. Mater. Chem. A* **2015,** *3*, 555-561.